Article:
Kupai, MM, Yang, F, Harbottle, D et al. (3 more authors) (2013) Characterising rag-forming solids. Canadian Journal of Chemical Engineering, 91 (8). 1395 - 1401. ISSN 0008-4034

https://doi.org/10.1002/cjce.21842

Characterizing rag-forming solids

Morvarid Madjlessi Kupai[1], Fan Yang[1], David Harbottle[1], Kevin Moran[2], Jacob Masliyah[1] and Zhenghe Xu[1]

[1]Department of Chemical and Materials Engineering, University of Alberta, Canada

[2]Titanium Corporation, Suite 1400, Baker Centre, 10025-106 Street, Edmonton, Alberta, Canada

Abstract

In oil sands froth treatment an undesirable intermediate layer often accumulates during the separation of water-oil emulsions. The layer referred to as 'rag' is a complex mixture of water, oil, solids and interfacially active components. The presence of a rag layer has a detrimental impact on separation of water and fine solids from diluted bitumen. The current study focuses on characterization of solids from a rag layer forming stream of a naphthenic froth treatment plant in an attempt to understand the mechanism of rag layer formation. Through detailed characterization of rag-forming and non-rag-forming solids, the mineralogy of solids and their contamination were shown to be critical to rag layer formation. The iron-based minerals such as siderite and pyrite were found to be enriched within the rag layer. Analysis of surface organic complexes confirms a high level of organic matter association with these solids through the binding of carboxylic acid group with iron on solids, resulting in a surface hydrophobicity susceptible for rag layer formation.

Keywords: Rag layer, Iron-based minerals, Organic matter

Introduction

In Northern Alberta, oil sand deposits continue to provide a source of energy for Canada and the surrounding territories. Over the last 40 plus years the oil sand deposits have been successfully mined to extract bitumen trapped within a complex mineral network. The Clark Hot Water based Extraction processes have been exclusively used by oil sand operators to recover bitumen from mineable oil sands. The mined ore is pre-conditioned in a hydrotransport pipeline with injection of chemical additives (often sodium hydroxide) and air to promote the liberation and aeration of bitumen droplets. In the primary separation vessel, air bubbles engulfed in bitumen rise to the top of the separation vessel, forming a froth composed of typically 60% bitumen, 30% water and 10% solids (predominately fines, $< 44\mu m$) by mass. The bitumen froth is subsequently diluted with solvent, either naphtha or paraffinic diluents, to lower the viscosity of bitumen and increase the density difference between the two liquid phases (diluted bitumen and water). Enhanced separation is achieved through the use of inclined plate settlers, cyclones and/ or centrifuges. During the separation it is not uncommon to observe the accumulation of a viscous layer that reduces dewatering efficiency. The viscous layer is often referred to as 'rag' and is a complex mixture of water, diluted bitumen, fines, and interfacially active chemical species (asphaltenes, surfactants, etc.).

The exact composition and formation mechanism of rag layer has been debated in literature. Saadatmand et al. (2008) described the rag-material to be an oil continuous layer containing emulsified water and solid particles. Complex fluids of water-in-oil emulsions, solids-in-oil dispersions, oil-in-oil dispersions, and oil-in-water-in-oil multiple emulsions have been reported by Varadaraj and Brons (2007) and Czarnecki et al. (2007) when studying water in crude oil and diluted bitumen emulsions, respectively.

Rag layer stability is often attributed to the combination of fine particles and surface active species such as asphaltenes which irreversibly adsorb at the oil-water interface, forming interfacial films that are resistant to coalescence. (Rane et al., 2012; Yeung et al., 1999) Using a modified micropipette technique, Yeung et al. (2000) showed that a water droplet formed in 0.1 wt% bitumen diluted heptol was extremely stable against coalescence and a rigid interfacial film that crumpled abruptly upon droplet deflation was responsible for such high stability of water in diluted bitumen emulsions. At higher bitumen concentrations (10 wt%) the film appeared much more flexible with the droplet retaining its spherical shape upon deflation. The transition in rigidity of interfacial films is most likely associated with the ratio of interfacially active species partitioned at the water-oil interface. For example, while being more surface active than asphaltenes, maltenes alone do not form a rigid interfacial film and act to reduce the rigidity of the interfacial layer. (Gao et al., 2009, 2010; Tchoukov et al., 2010) Interfacial rigidity is also known to correlate with solvent aromaticity, with the elasticity of the interfacial films being a function of asphaltene solubility. (Spiecker and Kilpatrick, 2004) The rigidity of the film is an important parameter in stabilizing interfacial films, since it is governed by the formation of a continuous network at the interface that exhibits a yield strength apposing film rupture.

Stabilization of interfacial films by solid particles has been considered in detail since the work of Pickering (1907). Similar to surfactants in which stability is associated with the HLB index, fine particles and their stabilizing potential at an oil-water interface is dependent on wettability or contact angle of the solids at the liquid-liquid interface.(Binks, 2002) While hydrophilic particles (contact angle θ measured through aqueous phase $< 90^{o}$) stabilize oil-in-water emulsions, hydrophobic particles ($\theta > 90^{o}$) stabilize water-in-oil emulsions. Assuming that the particles are small enough such that the gravitational contribution can be neglected, the stability of an

emulsion is shown to correlate with the particle detachment energy (E) from the interface given by:

$$E = \pi r^2 \gamma_{\alpha\beta}(1 \pm cos\theta)^2 \quad [1]$$

where r is the particle radius, $\gamma_{\alpha\beta}$ is the water-oil interfacial tension, and $\pm$ defines the removal of the particle into the water (negative) and oil (positive) phases. Based on equation 1, the maximum detachment energy is obtained when θ = 90^o. (Binks, 2002)

When in contact with aqueous solutions natural surfactants (naphthenic acids) are released from bitumen with the potential to generate very stable emulsions when in the lamellar liquid crystal phase. (Horvath-Szabo et al., 2001, 2003) In the presence of fine solids, the interaction of sodium naphthenates with kaolinite particles can also impact the stability of emulsions with the naphthenates acting as a modifier of solid wettability. (Jiang et al., 2011b) Bi-wettable solids can result in localized phase inversion, creating multiple emulsions of oil-in-water-in-oil or vice versa. (Binks and Lumsdon, 2000) These emulsions are most problematic since the apparent density of the droplet becomes intermediate to both fluid phases, making emulsion separation by sedimentation or creaming extremely difficult if not impossible.

In oil sands processing there is an assembly of surface active species that have the potential to form stable droplets of intermediate density that lead to the gradual formation of a rag layer. However, in the absence of fines the addition of an appropriate chemical demulsifier or coalescer is often sufficient to achieve almost complete separation and prevent the formation of a rag layer. (Jiang et al., 2008; Jiang et al., 2011a) Hence the fines are a critical component in rag layer formation and stabilization. The objective of the current study is to identify the type of minerals

critical to the formation of a rag layer, and their associated surface characteristics that govern such stability.

Materials and methods

In the current study, a sample from the secondary cyclone overflow of a naphthenic froth treatment plant experiencing rag layer accumulation was investigated. Due to sampling and sample handling issues the rag layer was regenerated from the sample in the laboratory using a mechanical shaker. After 30 minutes of shaking the sample was gently transferred to a 100-mL graduated cylinder, sealed tightly with Parafilm® and left to stand at room temperature for 14 days. After 14 days the sample was observed to form a thin oil layer (nearly solids and water free), an aqueous phase concentrated with fines, and a viscous middle layer that could be described as rag. The rag layer itself accounted for a significant proportion of the cylinder volume, considerably reducing the volume of the oil phase.

Solids characterization: Solids at various locations along the cylinder were collected carefully using a wide-tip pipette, ensuring minimum disturbance and avoiding potential mixing of the layers. The recovered solids were cleaned prior to characterization. Two levels of cleaning were employed; i) toluene washing to remove any toluene soluble organics and ii) low temperature ashing to remove the remaining organic matter. Once recovered, the solid samples were dispersed in toluene, mixed for 30 mins and then centrifuged at 20,000 g for 25 mins to separate the solids from the liquid. The washing process was repeated several times until the supernatant appeared clear. The resultant solids were then dried in a vacuum oven at 40^{o}C for 24 hrs to remove any remaining solvent. In order to accurately determine the mineralogy of the solids by

X-ray diffraction, low temperature ashing (plasma asher K1050X [Quorum Emitech, England]) was employed to remove any remaining organic matter. Low temperature ashing uses a radio frequency radiation to dissociate, ionize and excite oxygen molecules into chemically excited atoms which are used to remove organic matter from samples. The process was carried out at a low pressure of 0.6 mbar, with combustion products being removed by a vacuum system.(Adegoroye et al., 2009)

X-Ray Diffraction (XRD) analysis: A Bruker D8 Advance (Bruker AXS, Inc., USA) equipped with an incident beam parabolic mirror for cobalt radiation (CoKα) and a linear detector (VANTEC-1™) was used to obtain diffraction patterns of the minerals. Sub-micron/ micron size solids were dispersed in distilled water and transferred onto a quartz plate by the addition of a few drops of solid dispersion. Low temperature heating was applied to evaporate the water prior to each measurement. Quantification of the mineral phases present in the random minerals was obtained with TOPAS™. The technique relies upon multiphase structure refinement (Rietveld) to give the weight percent of minerals present. Model structures were taken from the Inorganic Crystal Structure Database (ICSD). (Adegoroye et al., 2010)

Fourier Transform Infrared Spectroscopy (FTIR): Infrared spectra of the minerals were obtained using a Bio-Rad FTS 6000 (Bio-Rad, USA). The toluene washed solids were dispersed in KBr to a concentration of 2.6 wt%. The mixture was placed in a sample holder for absorbance measurement. The spectra were acquired at 4 cm^{-1} resolution over the mid-IR spectral region. (Adegoroye et al., 2010)

Film flotation technique: The wettability of solids was pseudo-quantitatively measured using the film flotation method of Fuerstenau et al. (1991). A critical surface tension is defined by the

highest surface tension of the liquid that completely wets the solids. Using water/ alcohol (ethanol) solution as the probing liquid, the surface tension can be controlled by increasing the alcohol to water ratio. A critical surface tension distribution of solids can be determined by measuring the mass fraction of solids residing on the liquid surface of different surface tensions. A higher mean critical surface tension indicates the solids being less hydrophobic. For wettability measurement, solids from aqueous phase and rag layer were cleaned using excess toluene and dried prior to being gently sprinkled onto the liquid interface. Toluene washing is intended to remove loosely bound toluene soluble organic matters without removing tightly bound toluene soluble organic matters. The toluene washing is therefore considered not detrimental for the purpose of characterizing the wettability of fines even though it may not represent the natural state of the solids in various streams.

Water drop penetration test: The technique relies upon measuring the time required for a de-ionized water droplet to completely penetrate into a solid pellet. The penetration time provides a relative measure of solids wettability, with short (seconds) and long (minutes) penetration time corresponding to hydrophilic and hydrophobic solids, respectively. To minimize error associated with pellets of differing pore sizes (particle size effect) the solids collected were screened at 44 μm. Each pellet was prepared using 5 g of solids transferred into a die cast and compacted under a loading force of 9000 psi for 4 mins (hydraulic press: Enerpac JH-5). Using a KRÜSS drop shape analysis system (DSA 10, KRÜSS GmbH, Germany), images of a 40 μL de-ionized water drop penetrating into the solid pellet were recorded at a rate of 0.5 fps.

Results and discussion

Rag-layer properties

A regenerated rag layer was observed to remain stable in excess of 3 months. The rag layer formed on the aqueous phase, suggesting an oil continuous layer. To confirm the nature of this layer a small drop of the rag layer was placed in both naphtha and water. In naphtha the rag drop was observed to diffuse/ disperse rapidly, while in water the rag drop remained its original shape while rising to the air-water interface. Such observations led us to conclude the rag layer as oil continuous.

Optical microscopy was used to further elucidate the nature of the rag layer. In this case, samples were pipetted onto microscope slides and imaged using a Carl Zeiss Axioskop 40 Pol microscope (Zeiss, Germany). Figure 1a and 1b show images of a sample recovered from the nearly solids free oil layer above the rag layer (Figure 1a), and a sample of the rag layer (Figure 1b).

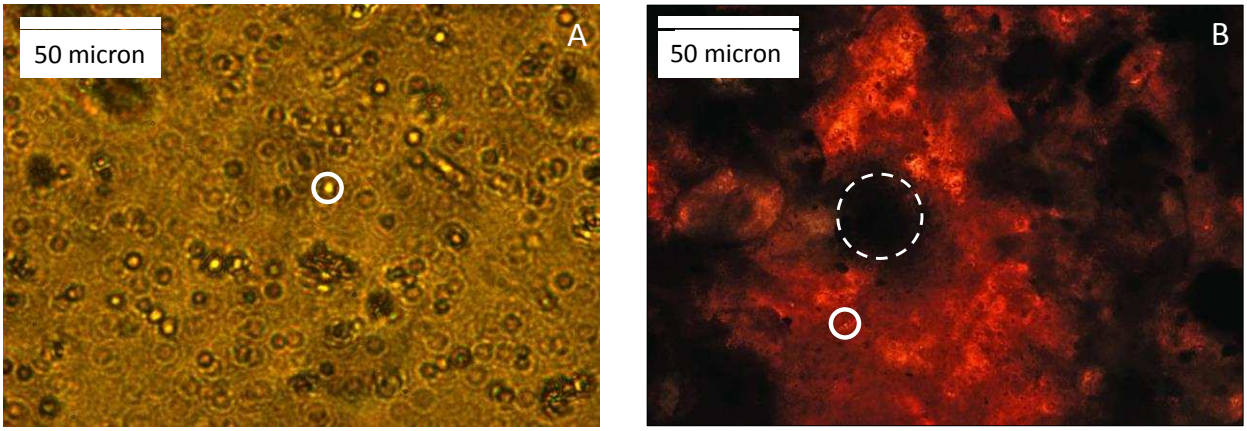

Figure 1 Optical microscope image of a sample removed from the oil layer (A) and the rag layer (B).

Micron sized water droplets (solid circle) were observed within the oil phase. Flocs of water droplets were not clearly visible; most likely due to low water content of the samples, see Figure 4. The darker regions of spherical shape in Figure 1a is most likely water droplets stabilized by fines or bituminous species. This was supported by a measurable amount of water (3.1 wt%) in the organic phase determined by Karl Fischer titration. The solids content in the oil phase was unmeasurable in the small volume of oil recovered and considered negligible. Figure 1b shows an image of the rag layer extracted from a position 3 cm below the oil-rag interface. Individual water droplets were observed once again (solid circle), but the nature of the layer becomes much more complex. Dense black regions (dashed circle) appear somewhat interconnected, with lighter diffuse regions occupying the remainder of the volume. To better understand the system, dilution experiments were conducted in which either heptane (Figure 2a) or toluene (Figure 2b) was gradually added dropwise onto the rag layer sample. Dilution continued by adding more solvent until the drained solvent (wash off from rag layer) appeared clear.

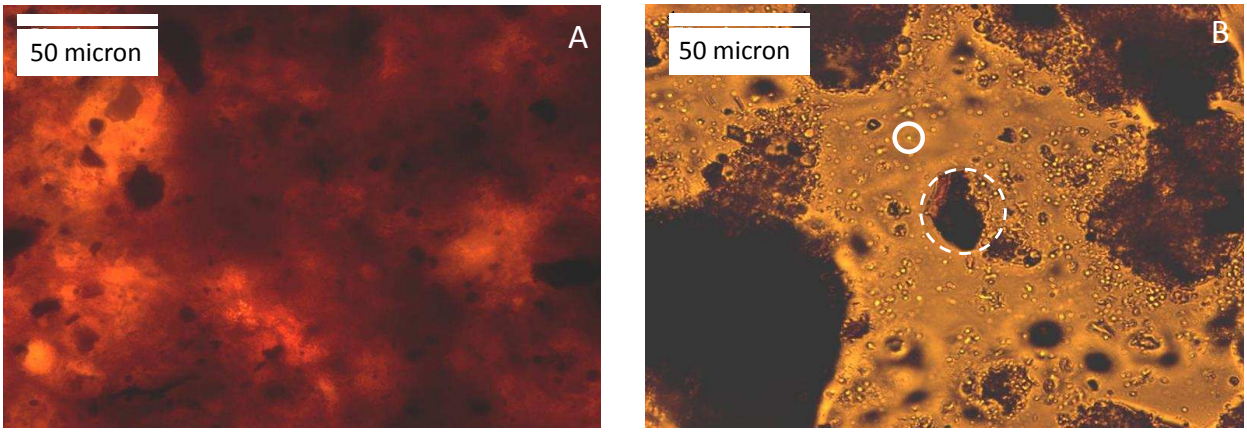

Figure 2 Optical microscope image of the rag layer sample heptane washed (A) and toluene washed (B).

Interestingly, in the case of heptane the diluted rag layer appeared unchanged. A very murky sample remained composed of both diffuse and dense black regions, similar to the untreated rag layer sample in Figure 1b. However, the appearance of the sample by dilution with toluene was significantly different. A large proportion of the sample was washed away in the excess solvent, revealing micron sized water droplets dispersed and flocculated throughout the continuous oil phase, but there remained dense black regions. Dilution experiments confirmed that much of the rag layer material was soluble in aromatic solvents, and the dense black regions appear resistant to even toluene washing. While the diffuse regions appear to be composed of bituminous components, either free or solid associated, the dark regions appear to be dense flocs (aggregates) of fines.

The physical properties (apparent density, solids content and water content) of the rag layer were investigated by sampling at various depths along the cylinder. Using a wide tip pipette, a small sample was extracted at each sampling height and the apparent density of the sample measured using an Anton Paar DMA 38 density meter (Anton Paar, USA) at room temperature. The apparent density profiles throughout the oil layer and rag layer are shown in Figure 3. The density of oil layer was measured to be 0.88 g/cm^3, slightly higher than 0.86 g/cm^3 measured for a solids and water free oil sample.

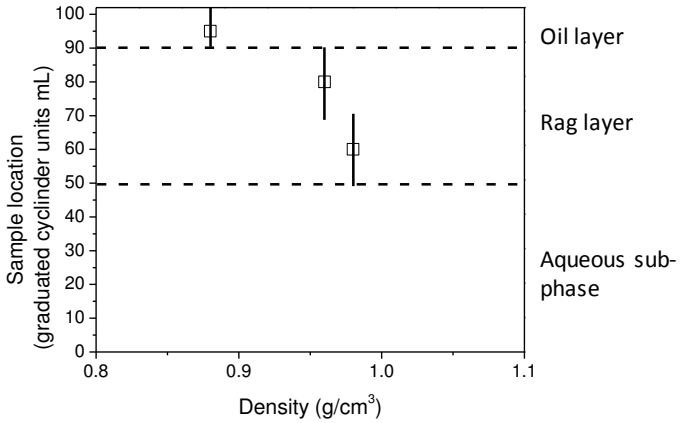

Figure 3 Density profile through the oil and rag layers.

An increase in the overall density of the samples collected from the top towards the rag-water interface was measured. The density of samples collected from the top and bottom of the rag layer was measured to be ~0.96 g/cm3 and ~0.98 g/cm3, respectively. Such densities are intermediate to the two liquid phases and solids, supporting the discussion on the formation of an intermediate density middle layer.(Czarnecki et al., 2007) It is important to note that the density measured represents just an overall density of the samples collected. It does not represent the density of any single phase, but provides an indication of the composition (solids, water and oil content) of the sample.

Figure 4 shows the water and solids contents in the extracted samples. Water content was determined by Karl Fischer titration and solids content determined by dry mass analysis after washing of the sample with excess of solvent (toluene).

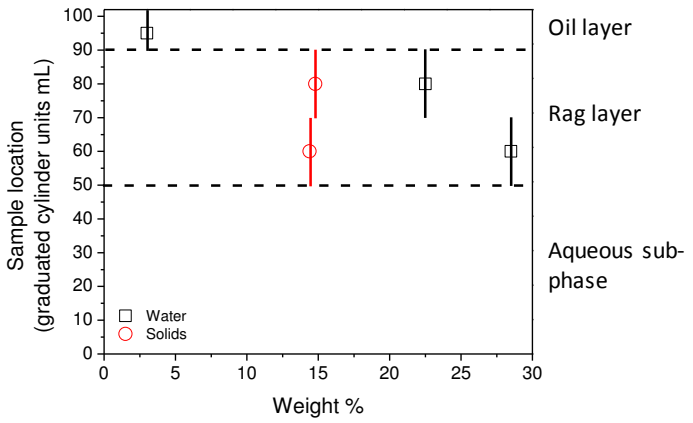

Figure 4 Solids and water content profile through the rag layer.

The water content in the oil layer was approximately ~3 wt%, which in addition to the fines (Figure 1a) would account for the 0.02 g/cm^3 density increase with respect to the solids and water free oil. The water content in the rag layer varies between 22.5 – 28.5 wt% which represents a significant quantity of trapped water. Greater water loading closer to the rag-water interface indicates the slow coalescence of water droplets with the aqueous sub-phase and their accumulation. Smaller and slower settling droplets would remain dispersed and become trapped in the rag layer, with a decreased loading towards the rag-oil interface. Interestingly, the solid content appears to show little variation throughout the rag layer, remaining at ~14.5 wt%. Such characteristic may result from the partitioning of particles at the water-oil interface (particle stabilized droplets) and a uniform interfacial area throughout the rag layer. Alternatively, it may result from the formation of a gel-like structure that is able to resist solids migration due to their self-association and association at the water-oil interface. The high viscoelastic nature of rag layer material compared with particle-free oil has been confirmed by Varadaraj and Brons (2007). A characteristic of gel-forming particles is a greater degree of organic-mineral complexation, which has been confirmed by Salehi (2010) who studied the structure forming

behavior of organic coated particles recovered from mature fine tailings. From the current analysis, rag layer formation is clearly undesirable. Not only does the rag layer form an impenetrable layer that prevents effective separation, (Czarnecki et al., 2007) but its total mass is composed of nearly two-thirds of solbit (solvent diluted bitumen), the sought after product in separation.

Particle characterization

Particle size distribution: Figure 5 shows the particle size distribution of the solids obtained from the rag and aqueous phases (data collected using a Mastersizer 2000; Malvern Instruments, UK). After carefully collecting the rag and aqueous phases, all the solids in each phase were separated and cleaned using toluene and low temperature ashing following the procedures described in the experimental section. To accurately measure the particle size distribution, particle aggregation needs to be avoided, which was accomplished by adding sodium silicate to the suspension and applying a moderate sonication prior to each measurement. The results obtained as such show that the solids in the rag layer are slightly smaller than the solids in the aqueous phase. The solids in the rag layer are all fines (< 44 μm), while the solids in the aqueous phase contains a significant amount of coarse material. Both samples contain a significant amount of clays (< 2 μm). Although the coarse solids are known of less potency to stabilize emulsions (Binks and Lumsdon, 2001; Lopetinsky et al., 2006), the difference in particle size distribution alone does not appear to be the reason for rag layer formation since a high percentage of solids recovered from both phases (number basis) are of sub-micron sizes.

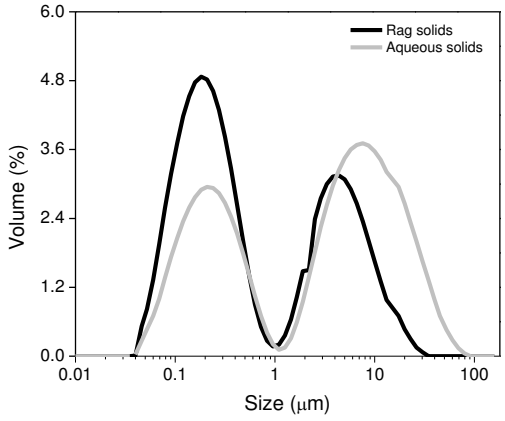

Figure 5 Particle size distributions of solids collected from the aqueous phase and rag layer.

Wettability of solids: Figure 6 shows the floatability of the solids extracted from the rag layer and aqueous phase. In pure water (γ = 72.8 mN/m) 100% of the solids from rag layer floated, in contrast to ~84% for the solids from aqueous phase. The 16% solids sunk are most likely hydrophilic coarse solids residing in the aqueous phase. In lowering the surface tension by the addition of ethanol, 100% of the solids from the rag layer floated until a surface tension of 52 mN/m, defined as the upper critical surface tension of wetting, γ_c^{max}. With further reduction in surface tension of the probing liquid, the fraction of solids floating reduced until the surface tension of the probing liquid reaches 25 mN/m, at which all the particles sank into the probing liquid. The surface tension is defined as the lower critical surface tension of wetting, γ_c^{min}. The lower critical surface tension for the solids from aqueous phase was determined to be 30 mN/m. The critical surface tension distribution of the solids from the aqueous phase is shifted to the right of the distribution for the solids from the rag layer, suggesting that the solids in the aqueous phase are less hydrophobic than the solids from the rag layer. The wettability of solids is recognized as an important parameter in stabilizing emulsions, with oil-wet solids readily

stabilizing water-in-oil emulsions. A greater quantity and stronger hydrophobicity of the solids in the rag layer appears to support the formation of the rag layer.

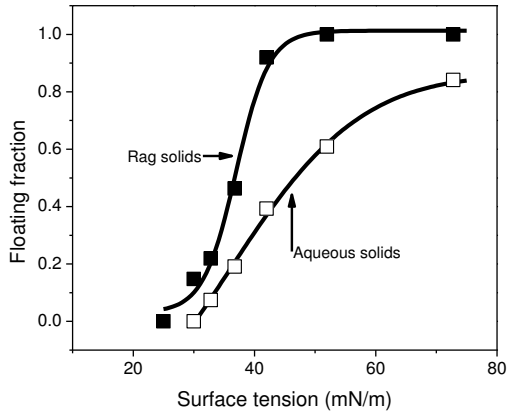

Figure 6 Fraction of particles floating as a function of probing liquid surface tension.

Surface contamination: The association of organic matter with the solids collected from the aqueous phase and rag layer was studied using FTIR. For the simplicity of discussion the data are divided into the following spectral regions; 800 – 1550 cm^{-1}, 1550 – 1750 cm^{-1}, 2800 – 3500 cm^{-1} and 3600 – 3720 cm^{-1}, as shown in Figure 7. The bands at 3621 – 3698 cm^{-1} are characteristic of kaolinite clays, (Gu et al., 2007). For semi-quantitative analysis, the spectra are normalized with respect to these clay peaks.

The spectral feature in region 1600 – 1700 cm^{-1} is free of any interference from clays and is often considered the most informative when considering the association of organic matter. The shoulder at ~1700 cm^{-1} is assigned to the stretch of C=O which is visible for the solids from rag layer but not for the solids from the aqueous phase. Based on previous characterization of Athabasca asphaltene the 1700 cm^{-1} shoulder is likely ketones and the band at 1600 cm^{-1} represents aromatic ring stretch. (Wu, 2003) Bands at 2925 and 2856 cm^{-1} are attributed to

stretching and bending vibrations of aliphatic CH_2 and CH_3 groups (Gu et al., 2006) and the broad band at 3200 – 3400 cm^{-1} is characteristic of functional groups with nitrogen (R-NH2, Ar-NH2, R-NH-R, Ar-NH-R, where Ar represents aromatic ring carbon and R the aliphatic chain carbon) and hydrogen bonded O-H. (Gu et al., 2007; Gu et al., 2006) In the spectral regions 1550 – 1750 cm^{-1} and 2800 – 3500 cm^{-1} the bands are more intense for the solids recovered from the rag layer, indicating more organic matter associated with the solids in rag layer. The band at ~864 cm^{-1}, characteristic of siderite, (Schoonen et al., 2012) is of much higher intensity for the solids from the rag layer than that from the aqueous phase, suggesting the enrichment of siderite in the solids within the rag layer. The enrichment of siderite in the rag layer also accounts for a stronger broad band at ~1450 cm^{-1}, which is attributed to carbonate associated with siderite. (Adegoroye et al., 2010) Higher organic content of the solids in the rag layer supports stronger hydrophobicity of solids. Higher content of siderite in the rag layer appears to suggest that siderite is more contaminated and a key component responsible for rag layer formation. Strong contamination of siderite occurs most likely due to strong affinity of carboxylic acid groups of organic compounds in bitumen with iron on siderite.

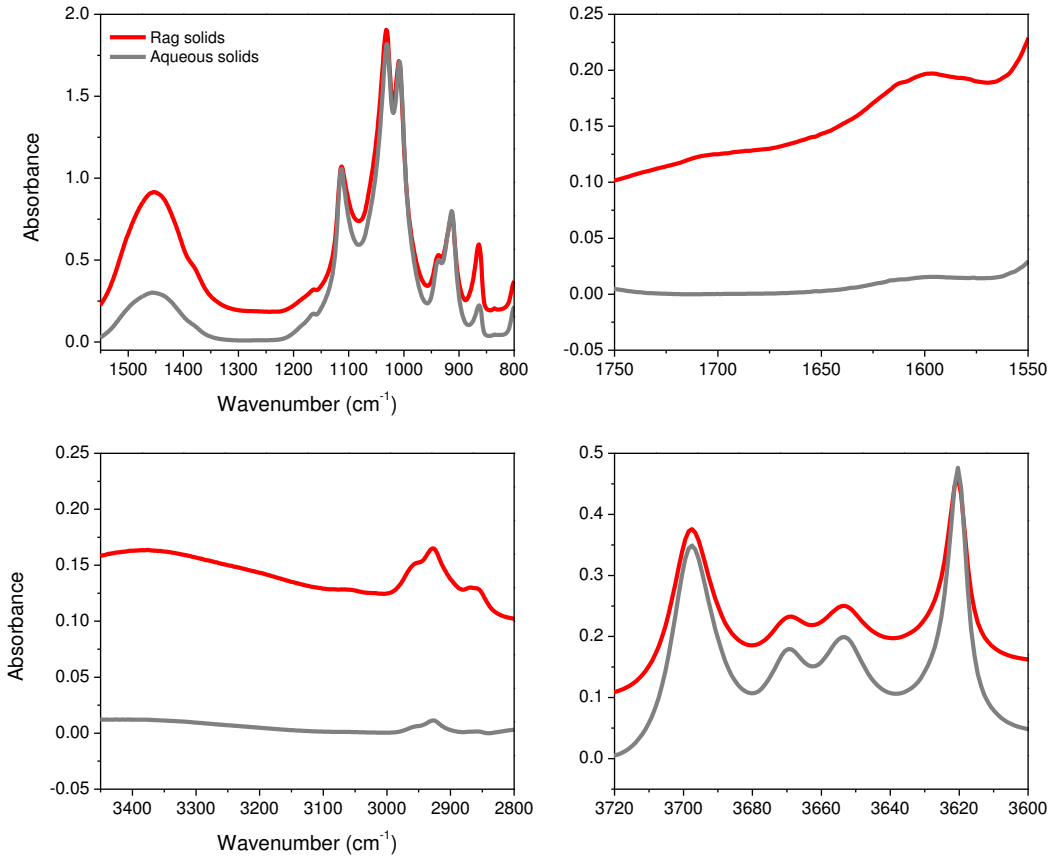

Figure 7 FTIR spectra of the aqueous and rag solids.

Mineralogy: Figure 8 compares the mineralogy of the solids collected from both the aqueous phase and rag layer. The two fingerprints are distinctly different. In the case of the solids from the aqueous phase, kaolinite and illite account for nearly 80 wt% of the sample. The high percentage of these two mineral phases is consistent with previous research studying the solids isolated from bitumen froth of different oil sand ores. (Adegoroye et al., 2010) Chlorite accounts for ~10 wt% of the mineral phases, with quartz and siderite each around 5 wt%. In contrast, the solids isolated from the rag layer contain substantially less kaolinite (~15 wt%) and substantially more siderite (~47 wt%) and pyrite (~11 wt%). The iron-bearing heavy minerals are shown to preferentially partition in the rag layer. It appears that these iron-bearing minerals are heavily

contaminated by organic matters and accumulate at oil-water interface due to their biwettable nature, stabilizing droplets and causing the formation of rag layer. The absorbance spectra in Figure 7 confirm that the solids from rag layer are highly contaminated with organic matter and hence more hydrophobic than the solids from the aqueous phase, in agreement with the wettability observations (Figure 6). Such characteristics would support the formation of a stable water-in-oil emulsion, but the question is posed about the enhanced stabilizing capacity of siderite and pyrite.

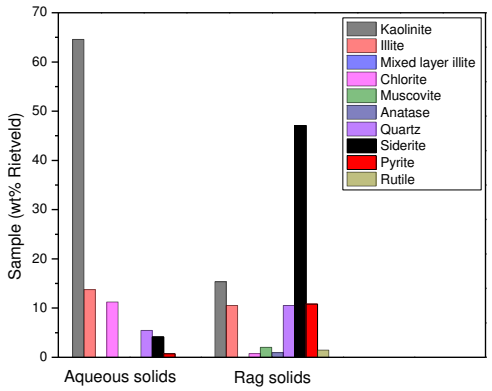

Figure 8 Mineral phases of solids from the aqueous phase and rag layer, determined by XRD.

Solids contamination: To further understand the contamination (organic-mineral complexation) and its role of solids in rag layer formation, contamination studies of kaolinite and siderite (minerals purchased from Ward's Natural Science, USA) were conducted. The kaolinite and siderite solids were ground to d_{50} ~ 3.2 μm and 7.7 μm, respectively. Contamination was accomplished by dispersing 5 g of solids in 120 mL diluted bitumen with a bitumen concentration of 10 g/L. The aromaticity of the solvent was varied (toluene, heptol 1:1, heptane) to study contamination in good and poor solvents. After shaking the suspension for 15 hrs, the

solids were centrifuged and washed with excess de-ionized water to remove any free hydrocarbon trapped in the voids of the solids. Figure 9 shows the results of the water drop penetration time measurement using the procedure described in the experimental section. For untreated particles (blank) the water drop penetration time for both minerals is less than 20 seconds, which confirms that the original minerals are hydrophilic. After mixing in solbit, kaolinite particles became slightly more hydrophobic. The water drop penetration time of solids contaminated in various solvent-diluted bitumen increased in the order blank < toluene < heptol < heptane. Mixing in heptane diluted bitumen increased the water drop penetration time to ~63 sec. For siderite, the water drop penetration time for the untreated and toluene soaked solids could be considered the same within experimental error, showing little variation in wettability. However, unlike kaolinite, siderite shows nearly an order of magnitude increase in the water drop penetration time after exposure to heptol and heptane diluted bitumen. Treated with heptol and heptane diluted bitumen, the water drop penetration time of solids increased to ~170 and ~ 250 sec, respectively. Such an increase represents a marked change in wettability with the solids being considered hydrophobic. The preferential association of organic matter with siderite has been attributed to strong linkage between carboxylic acids of organic compounds in bitumen and iron on siderite. Readers are referred to the following publications for a more in-depth discussion. (Suess, 1970, 1973; Vandegrift et al., 1980)

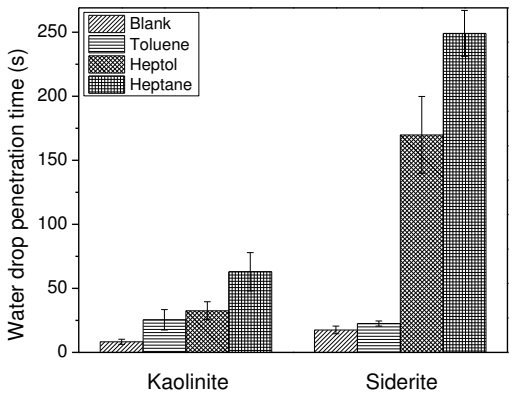

Figure 9 Water drop penetration times of kaolinite and siderite contaminated by diluted bitumen.

Conclusions

The rag layer is identified as oil continuous composed of water droplets, fine solids and organic matter. A continuous gel-like network of fine solids throughout the layer is able to resist consolidation, trapping the liquid phases within. The rag solids are hydrophobic which supports the notion that hydrophobic particles stabilize water-in-oil emulsions. The stronger hydrophobicity is related to greater organic-mineral complexation. X-ray diffraction study points to a high level of heavy minerals such as siderite and pyrite accumulating in the rag layer, supported by the results of FTIR characterization. Contamination studies confirmed that siderite readily associates with organic matter in bitumen.

While siderite and pyrite account for a small fraction of the total minerals floated during bitumen extraction, (Adegoroye et al., 2010) their presence seems to become more prominent during froth treatment as the mineralogy of the sample shifts. These hydrophobic, structure-forming fines up to 40% of total solids in the rag layer eventually predominate in the system and provide favorable conditions for rag layer formation.

Acknowledgements

We thank the Natural Sciences and Engineering Research Council of Canada (NSERC) Industrial Research Chair Program in Oil Sands Engineering for the financial support and Canadian Natural Resources Ltd. for the froth samples.

References

Adegoroye, A., Uhlik, P., Omotoso, O., Xu, Z., Masliyah, J., 2009. A Comprehensive Analysis of Organic Matter Removal from Clay-Sized Minerals Extracted from Oil Sands Using Low Temperature Ashing and Hydrogen Peroxide. Energy & Fuels 23, 3716-3720.

Adegoroye, A., Wang, L., Omotoso, O., Xu, Z., Masliyah, J., 2010. CHARACTERIZATION OF ORGANIC-COATED SOLIDS ISOLATED FROM DIFFERENT OIL SANDS. Canadian Journal of Chemical Engineering 88, 462-470.

Binks, B.P., 2002. Particles as surfactants - similarities and differences. Current Opinion in Colloid & Interface Science 7, 21-41.

Binks, B.P., Lumsdon, S.O., 2000. Transitional phase inversion of solid-stabilized emulsions using particle mixtures. Langmuir 16, 3748-3756.

Binks, B.P., Lumsdon, S.O., 2001. Pickering Emulsions Stabilized by Monodisperse Latex Particles: Effects of Particle Size. Langmuir 17, 4540-4547.

Czarnecki, J., Moran, K., Yang, X., 2007. On the "rag layer" and diluted bitumen froth dewatering. Canadian Journal of Chemical Engineering 85, 748-755.

Fuerstenau, D.W., Diao, J., Williams, M.C., 1991. CHARACTERIZATION OF THE WETTABILITY OF SOLID PARTICLES BY FILM FLOTATION .1. EXPERIMENTAL INVESTIGATION. Colloids and Surfaces 60, 127-144.

Gao, S., Moran, K., Xu, Z., Masliyah, J., 2009. Role of Bitumen Components in Stabilizing Water-in-Diluted Oil Emulsions. Energy & Fuels 23, 2606-2612.

Gao, S., Moran, K., Xu, Z., Masliyah, J., 2010. Role of Naphthenic Acids in Stabilizing Water-in-Diluted Model Oil Emulsions. Journal of Physical Chemistry B 114, 7710-7718.

Gu, G., Zhang, L., Xu, Z., Mashyah, J., 2007. Novel bitumen froth cleaning device and rag layer characterization. Energy & Fuels 21, 3462-3468.

Gu, G.X., Zhang, L.Y., Wu, X.A., Xu, Z.H., Masliyah, J., 2006. Isolation and characterization of interfacial materials in bitumen emulsions. Energy & Fuels 20, 673-681.
Horvath-Szabo, G., Masliyah, J.H., Czarnecki, J., 2001. Phase behavior of sodium naphthenates, toluene, and water. Journal of Colloid and Interface Science 242, 247-254.
Horvath-Szabo, G., Masliyah, J.H., Czarnecki, J., 2003. Emulsion stability based on phase behavior in sodium naphthenates containing systems: Gels with a high organic solvent content. Journal of Colloid and Interface Science 257, 299-309.
Jiang, T., Hirasaki, G.J., Miller, C.A., Moran, K., 2008. Using Silicate and pH Control for Removal of the Rag Layer Containing Clay Solids Formed during Demulsification. Energy & Fuels 22, 4158-4164.
Jiang, T., Hirasaki, G.J., Miller, C.A., Ng, S., 2011a. Effects of Clay Wettability and Process Variables on Separation of Diluted Bitumen Emulsion. Energy & Fuels 25, 545-554.
Jiang, T., Hirasaki, G.J., Miller, C.A., Samson, N., 2011b. Wettability Alteration of Clay in Solid-Stabilized Emulsions. Energy & Fuels 25, 2551-2558.
Lopetinsky, R.J.G., Masliyah, J., Xu, Z., 2006. Solids Stabilized Emulsions: A Review. Colloidal Particles at Liquid Interfaces Cambridge University Press.
Pickering, S.U., 1907. Journal of the Chemical Society 91, 2001.
Rane, J.P., Harbottle, D., Pauchard, V., Couzis, A., Banerjee, S., 2012. Adsorption Kinetics of Asphaltenes at the Oil-Water Interface and Nanoaggregation in the Bulk. Langmuir 28, 9986-9995.
Saadatmand, M., Yarranton, H.W., Moran, K., 2008. Rag Layers in Oil Sand Froths. Industrial & Engineering Chemistry Research 47, 8828-8839.
Salehi, M., 2010. Characterization of mature fine tailings in the context of its response to chemical treatment. MSc thesis. University of Alberta.
Schoonen, M.A.A., Sklute, E.C., Dyar, M.D., Strongin, D.R., 2012. Reactivity of sandstones under conditions relevant to geosequestration: 1. Hematite-bearing sandstone exposed to supercritical carbon dioxide commingled with aqueous sulfite or sulfide solutions. Chemical Geology 296, 96-102.
Spiecker, P.M., Kilpatrick, P.K., 2004. Interfacial Rheology of Petroleum Asphaltenes at the Oil-Water Interface. Langmuir 20, 4022-4032.

Suess, E., 1970. INTERACTION OF ORGANIC COMPOUNDS WITH CALCIUM CARBONATE .1. ASSOCIATION PHENOMENA AND GEOCHEMICAL IMPLICATIONS. Geochimica Et Cosmochimica Acta 34, 157-&.

Suess, E., 1973. INTERACTION OF ORGANIC COMPOUNDS WITH CALCIUM-CARBONATE .2. ORGANO-CARBONATE ASSOCIATION IN RECENT SEDIMENTS. Geochimica Et Cosmochimica Acta 37, 2435-2447.

Tchoukov, P., Czarnecki, J., Dabros, T., 2010. Study of water-in-oil thin liquid films: Implications for the stability of petroleum emulsions. Colloids and Surfaces a-Physicochemical and Engineering Aspects 372, 15-21.

Vandegrift, G.F., Winans, R.E., Scott, R.G., Horwitz, E.P., 1980. QUANTITATIVE STUDY OF THE CARBOXYLIC-ACIDS IN GREEN RIVER OIL-SHALE BITUMEN. Fuel 59, 627-633.

Varadaraj, R., Brons, C., 2007. Molecular origins of crude oil interfacial activity part 3: Characterization of the complex fluid rag layer formed at crude oil-water interfaces. Energy & Fuels 21, 1617-1621.

Wu, X., 2003. Investigating the stability mechanism of water-in-diluted bitumen emulsions through isolation and characterization of the stabilizing materials at the interface. Energy & Fuels 17, 179-190.

Yeung, A., Dabros, T., Czarnecki, J., Masliyah, J., 1999. On the interfacial properties of micrometre-sized water droplets in crude oil. Proceedings of the Royal Society of London Series a-Mathematical Physical and Engineering Sciences 455, 3709-3723.

Yeung, A., Dabros, T., Masliyah, J., Czarnecki, J., 2000. Micropipette: a new technique in emulsion research. Colloids and Surfaces a-Physicochemical and Engineering Aspects 174, 169-181.